Journal of Cleaner Production 234 (2019) 1082–1093

Contents lists available at ScienceDirect

Journal of Cleaner Production

journal homepage: www.elsevier.com/locate/jclepro

Energy, exergy, advanced exergy and economic analyses of hybrid polymer electrolyte membrane (PEM) fuel cell and photovoltaic cells to produce hydrogen and electricity

M. Shaygan [a], M.A. Ehyaei [a, *], A. Ahmadi [b], M. El Haj Assad [c], José Luz Silveira [d]

[a] Department of Mechanical Engineering, Pardis Branch, Islamic Azad University, Pardis New City, Iran
[b] School of New Technologies, Iran University of Science & Technology, Iran
[c] Sustainable & Renewable Energy Engineering Department, University of Sharjah, United Arab Emirates
[d] São Paulo State University, UNESP, FEG, Energy Department, United Arab Emirates

ARTICLE INFO

Article history:
Received 27 May 2019
Received in revised form
24 June 2019
Accepted 26 June 2019
Available online 28 June 2019

Handling Editor: Sandro Nizetic

Keywords:
Photovoltaic cells
Exergy
Economic
Advances
Fuel cell
Electrolysis

ABSTRACT

Hydrogen, as a clean fuel, can provide all the requirements and characteristics of a clean and reliable energy carrier in the long term as a suitable alternative to fossil fuels. In this paper, a power generation system using hydrogen storage has been investigated. For this purpose, 64 photovoltaic modules with area of 2.16 m^2 for each module and 329 PW and 5.5 kW PEM fuel cell and electrolyzer were used in this hybrid system. The day product of hydrogen day has been calculated as 158 kg. The system has been subjected to exergy analysis and, hence the efficiency and destruction of exergy components have been calculated. The annual average electrical production by photovoltaic system is 4850 W. The average annual exergy efficiency of each component including compressor, electrolyzer, fuel cell, and photovoltaic cell has been calculated as 75.9%, 11.2%, 32.8%, and 10.8%, respectively. The energy and exergy efficiencies of the system have been calculated for different days and its average annual values have been obtained 20.4% and 21.8%, respectively. Cost of electricity is 0.127 $/kWh, which is compatible with solar thermal and wind turbine offshore electricity costs. Finally, according to the advanced exergy analysis in all equipment's except the photovoltaic cell, the highest exergy destruction has been related to exogenous unavoidable.

1. Introduction

Hydrogen as a clean fuel can be a suitable alternative to fossil fuels due to the fact that it has the characteristics of a clean and safe energy carrier in the long run, in addition to its highest energy per unit (Mitlitsky et al., 1998). The fuel cell and electrolysis unit's combination has become a new strategy for suppling the required hydrogen to the fuel cell for power generating unit. This combined system is the main source of power and applications in several units (Rekioua et al., 2014).

Hydrogen production for the use in fuel cells has been widely investigated. Bilgen (2004) examined various methods to produce hydrogen from renewable energy resource. A similar study was done be Levene et al. (2007) and Smaoui et al. (2015).

Integration of photovoltaic (PV) system with fuel cells has been recently investigated for the purpose of hydrogen production (Babayan et al., 2019). A new PV system integrated with polymer electrolyte membrane (PEM) fuel cell using phase change material (PCM) as a storage medium has been presented (Babayan et al., 2019) to produce hydrogen in a filling station of hydrogen. The study showed that the use of PCM resulted in an improvement of energy and exergy efficiencies of the proposed system.

Ashari et al. (2012) investigated a system consisting of PEM fuel cell, reformer, burner, and heat exchanger to provide the required electricity, heat and domestic hot water for a residential building. The study revealed that an 8.5 kW fuel cell could meet all the building loads requirements. Residential electricity cost was calculated to be 0.39 $/kWh which is considered to be a high electricity cost. This type of fuel cell was also investigated by Saidi et al. (Saidi et al., 2005a; Saidi et al., 2005b).

Hwang et al. (2009) examined the dynamic model of a hybrid fuel cell and photovoltaic cell system for residential applications.

* Corresponding author.
E-mail address: aliehyaei@yahoo.com (M.A. Ehyaei).

https://doi.org/10.1016/j.jclepro.2019.06.298
0959-6526/

The results showed that supplying electricity to a typical family was capable. Rekioua et al. (2014) examined a system of photovoltaic cells, PEM fuel cells, electrolyzer, and power control unit (PCU) as an independent system of the electrical grid. They used the PCU system for peak shaving and power consumption management.

The combination of a photovoltaic cell system, lithium battery and a PEM fuel cell was examined by Ezzat and Dincer (2016). They concluded that the system energy and exergy efficiencies for the combined fuel cell and battery were 39.5% and 56.3%, respectively and for the combined model of the fuel cell, battery and photovoltaic cell were 39.9% and 56.6%, respectively. Khemariya et al. (2017) developed a model for the optimal photovoltaic cell and a PEM fuel cell to provide electricity for a village in India. They used the hybrid optimization model carried out by electrical renewable (HOMER) software in order to select the optimal system.

Abadi et al., (Abadlia et al., 2017) investigated the control unit for a system included photovoltaic cell and fuel cell whereas it was connected to the grid. In the proposed system, photovoltaic (PV) cell was considered as a major power source and hydrogen fuel was the complimentary source. The power generated from PV ranges were consistent with the user's consumer load, as well as the production surplus for the electrolysis of water used for hydrogen production. The above system could switch to the network in parallel. Similar study was investigated by Dhabi et al. (Dahbi et al., 2018).

Baik et al. (2018) presented the scheme of solar and wind energy resources and seasonal energy reserves in Djanet (East - South Algeria). This study aimed to present an alternative solution to power generation in Djanet, mainly based on the diesel generator. Similar study has been done for Skyros, central region of Greece. The annual energy efficiency of this hybrid power plant is 19.7% (Petrakopoulou et al., 2016). The study of Bizon and Thounthong (2018) showed an optimal and subset of fuel cell hybrid power systems. It was on basis of the maximum power point (with and without the global capability).

Arsalis et al. (2018) investigated a system of the photovoltaic cell, water electrolysis, and fuel cell for supplying power for 100 families in Cyprus. According to the study, the cost of electricity was calculated as 0.216 EUR/kWh, which was currently more than the grid power price. The result of their research showed that if the operational life of fuel cell and electrolyzer was increased, with the reduction of photovoltaic cell prices, the electricity generated by this system could compete with the price of grid electricity.

Yadav and Banerjee (2018) studied the economic aspects of a system included solar electrical production system and electrolyzer. They found this system cannot compete with other hydrogen production methods.

Similar researches about the hybrid systems of wind turbine and photovoltaic systems to produce hydrogen were done by Maleki et al. (2016) and Silva et al. (Da Silva et al., 2005). Bukar and Tan (2019) investigated all of methods to produce hydrogen with renewable energy resources. They also reviewed the optimization techniques in this regard.

Instead of using PV to provide electricity for an electrolyzer, parabolic trough solar collector (PTC) was used for that purpose (Bagheri et al., 2019) where the electrolyzer fed a solid oxide fuel cell with hydrogen. The study revealed that PTC was a better option for the system due to the high operating temperature of the solid oxide fuel cell and the study also revealed that the highest exergy efficiency was about 27% and the minimum hydrogen levelized cost was 4.43 $/kg.

According to the above mentioned references in the literature, it can be stated no similar research has provided comprehensive research on energy, exergy and economic analyses simultaneously. In addition, there is no investigation in this regard for the location of the capital city of Iran (Tehran). Also, advanced exergy analysis of this system has not reported in the literature.

In this paper, electrolysis process is used to convert water into hydrogen and oxygen, and the produced hydrogen is stored in a storage tank at high pressure due to the use of compressor. The stored hydrogen is converted into electricity and steam by PEM fuel cell. Electricity needed by electrolysis system and compressor is supplied by photovoltaic cells. The main advantage of this proposed system is that it has no greenhouse gas emission during power generation process, and it also can be used locally for generating electricity in all kinds of residential and commercial buildings. The objective of this work is to investigate energy, exergy, economic and advanced exergy analyses in order find out the most suitable energy cost and efficient operating conditions for the society in Tehran city, Iran. According to the authors knowledge, advanced exergy efficiency has not been applied before for the proposed system. The work will serve the community with low economic income to implement such system of low electricity cost in order to solve the problem of high electricity bill paid by consumers.

The innovations of this paper include:

- Feasibility study of hybrid system for power and hydrogen production
- Energy, exergy, advanced exergy and economic analyses are presented
- Electricity cost is 0.127 $/kWh
- The highest hydrogen production is obtained 1420 kg/month in June.
- The highest exergetic efficiency are calculated as 8.2% in June.

2. Mathematical modeling

2.1. Energy analysis

Fig. 1 shows the schematic of the system where water is decomposed into hydrogen and oxygen by the electrolysis system. The produced hydrogen is stored in a storage tank and converted into electricity and steam in the PEM fuel cell. Meanwhile, the electricity required for the electrolysis system is supplied by photovoltaic cells.

The deflection angle (δ) is calculated by (John A. Duffie, 2013):

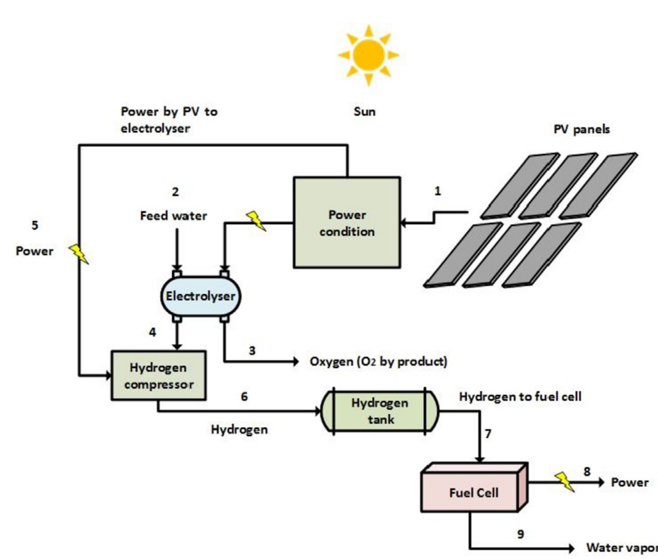

Fig. 1. Schematic diagram of the proposed system.

$$\delta = 23.45\sin\left(360\frac{284+n}{365}\right) \tag{1}$$

where n is the number of days.

The angle of incident beam of radiation is calculated by (John A. Duffie, 2013):

$$\cos\theta_z = \cos\varphi\cos\delta\cos\omega + \sin\varphi\sin\delta \tag{2}$$

In which, φ (Degree) is the latitude and ω (Degree) is the hour angle. For this hour angle, 1 h is equivalent to 15°.

In a similar relation, solar radiation is calculated by (John A. Duffie, 2013):

$$\dot{I}_b = S\sin\left(\frac{\pi}{2} - \theta_z\right) \tag{3}$$

where

$$S = G_{sc}\left(\bar{d}/d\right)^2 \tag{4}$$

$$\left(\frac{\bar{d}}{d}\right) = \frac{1}{(1 - 0.01673\cos(2n\pi/365))} \tag{5}$$

G_{sc} is a solar constant 1367 W/m^2.

The average amount of output power that can be obtained daily from the photovoltaic can be calculated by Bakelli et al. 2011:

$$\dot{E}_{array} = I_b\, A_{array}\, \eta_{pv}\, f_{man}\, f_{temp}\, f_{dirt}\, H_{tilt}\, N \tag{6}$$

where A_{array} (m^2) is the photovoltaic array area, η_{PV} is the photovoltaic array efficiency, $\dot{E}_{array}$ (W) is the average output power of the photovoltaic array, f_{man} is the error of the output power (W) of photovoltaic modules with an error of approximately ± 5% based on temperature of 25 °C for photovoltaic cells, f_{temp} is the e reduction factor due to increase of temperature, f_{dirt} is the reduction factor due to pollution, H_{tilt} is the radiation at sunrise hours for orientation and the specific collision angle which for Tehran is 5, N is the number of modules.

The amount of power reduction due to temperature increase can be calculated by Bakelli et al. 2011:

$$f_{temp} = 1 - \left(\gamma(T_{cell.eff} - 25)\right) \tag{7}$$

where γ (1/°C) is the temperature coefficient.

The current generated in the photovoltaic cells is a direct current (DC), so that a converter or inverter should be used to convert it to alternating current (AC). The converter output can be obtained from the manufactures catalog, usually converters have a conversion factor of 90–96%. A conversion factor of 92% is suggested, which is suggested for the efficiency of the equipment used to maximize the delivery capacity of the converter.

The system first law of thermodynamics is written:

$$\dot{Q}_{in} + \dot{W}_{in} + \sum_{in}\dot{m}h = \dot{Q}_{out} + \dot{W}_{out} + \sum_{out}\dot{m}h \tag{8}$$

where $\dot{Q}$ and $\dot{W}$ (W) are rates of the exchanged heat and work (between the control volume and the surrounding), respectively, h (J/kgK) is the specific enthalpy and $\dot{m}$ (kg/s) is the mass flow rate. The subtitles "in" and "out" refer to the input and output of these quantities between control volume and its surrounding.

The following chemical reactions occur at the anode and cathode of PEM fuel cell, respectively:

$$H_2 \rightarrow 2H^+ + 2e^- \tag{9}$$

$$2H^+ + \frac{1}{2}O_2 + 2e^- \rightarrow H_2O \tag{10}$$

Therefore, the fuel cell overall reaction is:

$$H_2 + \frac{1}{2}O_2 \rightarrow H_2O + \text{work} + \text{heat} \tag{11}$$

The energy conservation equation in the fuel cell is as follows:

$$\Delta H_{total} = H_{product} - H_{reactant} \tag{12}$$

where ΔH_{total} (kJ/kmol) is the maximum heat output from the fuel cell, calculated based on the difference between $H_{product}$ (kJ/kmol) enthalpy of the product and $H_{reactant}$ (kJ/kmol) enthalpy of reactant.

Due to changes of volumes, pressures and other irreversibility's in the fuel cell, the net output energy of the fuel cell is calculated by:

$$\Delta G = \Delta H_{total} - T\Delta S \tag{13}$$

where ΔG (kJ/kmol) is the maximum output of a fuel cell reaction (the motion of electrons in an external circuit), which is known as Gibbs free energy changes, ΔS (kJ/kmolK) is the change of entropy and T (K) is the temperature of the fuel cell. For the fuel cell reaction, the above equations can be conducted as follows:

$$\Delta\bar{g}_f = \bar{g}_f(\text{products}) - \bar{g}_f(\text{reactants}) \tag{14}$$

$$\Delta\bar{g}_f = \left(\bar{g}_f\right)_{H2O} - \left(\bar{g}_f\right)_{H2} - \frac{1}{2}\left(\bar{g}_f\right)_{O2} \tag{15}$$

The Gibbs free energy for the elements at the standard conditions (25 °C and 1 atm) is zero. If the fuel cell voltage is denoted by E, then following relation should be considered (Barbir and Gómez, 1997):

$$\Delta\bar{g}_f = -2FV_{rev} \tag{16}$$

where V_{rev} (V) is the reversible voltage of the fuel cell and F is Faraday constant and it is equal to 96475 C (Coulombs).

The fuel cell enthalpy is calculated by Barbir and Gómez 1997:

$$\Delta\bar{h}_f = -2FV_{theoretical} \tag{17}$$

where $V_{theoretical}$ (V) is the theoretical voltage of the fuel cell.

The output voltage of the fuel cell is derived from the following equation (Barbir and Gómez, 1997):

$$V_{FC} = V_{nernst} - V_{ohmic} - V_{activation} - V_{concentration} \tag{18}$$

where $V_{nernest}$ (V) is the fuel cell open - circuit voltage with no losses, which is calculated by Barbir and Gómez 1997:

$$V_{nernst} = \frac{\Delta G}{2F} + \frac{\Delta S}{2F}\left(T - T_{ref}\right) + \frac{RT}{2F}\left[\ln(P_{H_2}) + \frac{1}{2}\ln(P_{O_2})\right] \tag{19}$$

In the above equation, ΔG (J /mol) shows the change in Gibbs free energy, ΔS (J /molK) indicates that the change of entropy and P_{H_2} and P_{O_2} are the partial pressures of hydrogen and oxygen, respectively. The gas universal constant R is equal to 8.314 J /mol.K, T (K) is the fuel cell temperature and T_{ref} (K) is the reference temperature. The values of ΔG and ΔS are calculated based on standard temperature and pressure.

V_{ohm} (V) represents the resistance voltage drop which is called

Ohm resistance and it is derived from the following relation (Barbir and Gómez, 1997):

$$V_{ohm} = i_{FC}(R_M + R_C) \tag{20}$$

where R_C (Ω/cm) is the resistance of the electrodes against the passing of electrons. Also, R_M (Ω/cm) is the resistance of the electrolyte against the transit of ions and it is obtained from the following equations (Barbir and Gómez, 1997):

$$R_M = \rho_M \frac{L}{A} \tag{21}$$

$$\rho_M = \frac{181.6\left[1 + 0.03\left(\frac{i_{FC}}{A}\right) + 0.062\left(\frac{i_{FC}}{A}\right)^{2.5}\left(\frac{T}{303}\right)^2\right]}{\left[23 - 0.634 - 3\left(\frac{i_{FC}}{A}\right)\right]*\exp\left(4.18\left(\frac{T-303}{T}\right)\right)} \tag{22}$$

In which ρ_M (Ω.cm) is the specific resistance of the membrane, A (cm^2) is the fuel cell effective area and it is considered as 100 cm^2, L (cm) is the membrane thickness and i_{FC} (A/cm^2)is the current density of the fuel cell, which is assumed as 1.8.

V_{act} (V) indicates the reduction voltage of the activation in the electrode of anode and cathode and it is obtained from the following equation (Barbir and Gómez, 1997):

$$V_{act} = -\left[\zeta_1 + \zeta_2 T + \zeta_3 T\ln(C_{O_2}) + \zeta_4 T\ln(i_{FC})\right] \tag{23}$$

where

$$C_{O_2} = \frac{P_{O_2}}{5.08*10^{-6}\exp\left(-\frac{498}{T}\right)} \tag{24}$$

In the above equations, ξ is the geometrical parameters that they obtained based on the theoretical thermodynamic equations of electrochemical reactions. So, the values for ζ_1, ζ_2, ζ_3 and ζ_4 are −0.948, 0.0029, 0.000076 and −0.0000193,respectively. In addition, C_{O_2} (mol /cm^3) is the oxygen concentration at the catalysis surface.

V_{con} represents the concentration voltage drop and it is calculated by the following equation (Barbir and Gómez, 1997):

$$V_{con} = -\frac{RT}{2F}\ln\left(1 - \frac{J}{J_{max}}\right) \tag{25}$$

The value of J (current density) and J_{max} (maximum current density) are 3 and 1050 $mA/_{cm^2}$,respectively.

The consumed oxygen is usually supplied from the air. The amount of consumed hydrogen is obtained from the following equation (Barbir and Gómez, 1997):

$$M_{H2} = \frac{\dot{W}_{FC}}{2 \cdot V_{FC} \cdot \eta_{FC} \cdot F} \tag{26}$$

$$\dot{W}_{FC} = I_{FC} \cdot V_{FC} \cdot N_{FC} \tag{27}$$

where V_{FC} (V) is the output voltage, η_{FC} is the efficiency of the PEM fuel cell. This efficiency is assumed by 80%. $\dot{W}_{FC}$ (W) is the output power, N_{FC} is the number of plates.

For the mathematical modeling of PEM fuel cell, first V_{nernst} is calculated by equation (19), then the voltage losses (ohmic, activation and concentration) are calculated by equations (20)–(26). Real voltage of fuel cell is calculated by equation (18). Finally, the power production of fuel cell is calculated by equation (27).

The overall reaction in the electrolyzer as follows (Barbir and Gómez, 1997):

$$H_2O + \text{electricity} \rightarrow H_2 + \frac{1}{2}O_2 \tag{28}$$

The above chemical equation is used if the water entering the electrolyzer is fresh water. Due to the low hardness of water in Tehran. This item is ignored in this modeling.

The electrolyzer voltage efficiency is determined by the following equation (Barbir and Gómez, 1997):

$$\eta_V = \frac{1.25}{V_{elz}} \tag{29}$$

The efficiency of the voltage in this study is considered to be 74%. Therefore, the operational voltage value of the electrolyzer is equal to $V_{elz} = 2V$.

The hydrogen produced by the electrolyzer is calculated (Barbir and Gómez, 1997):

$$M_{H2} = \frac{\dot{W}_{elz}}{2 \cdot V_{elz} \cdot F} \tag{30}$$

In the above equation, M_{H2} (mole/s) indicates the molar rate of the produced hydrogen.

Power consumption of compressor is calculated by:

$$\dot{W}_c = C_p \cdot \frac{T_1}{\eta_C} \cdot \left(\left(\frac{P_6}{P_4}\right)^{\frac{k-1}{k}} - 1\right) \cdot \dot{m}_c \tag{31}$$

In the above equation, C_p (J/kgK) is the constant pressure specific heat capacity of hydrogen and it is 14320 J/kgK. T_1 (K) is the temperature of the hydrogen gas, which is considered 293 K P_4 and P_6 (Pa) are the input and output pressures in the compressor, respectively. k is the ratio of specific heat which is the isentropic expansion factor of hydrogen, η_C is the mechanical efficiency of the compressors is usually between 70% and 85% and $\dot{m}_c$ is mass flow rate of flow in the compressor (kg/s). The power of the compressor is supplied by photovoltaic cells.

The volume of the tank for a certain amount of hydrogen can be calculated:

$$V_{tank} = \frac{M_{tank} \cdot T_{tank} \cdot R}{P_{tank}} \tag{32}$$

In the above equation, M_{tank} (kg) and V_{tank} (lit) represent the stored mass and volume of the hydrogen in the tank. P_{tank} (Pa) and T_{tank} (K) are pressure and temperature of stored hydrogen and they are equal to 10 MPa and 293 K, respectively.

As electricity is produced by the DC fuel cell, a power regulation device converts the generated DC current into AC and also controls the current, voltage and output frequency. The efficiency of the power conversion device is typically 94%–98%.

2.2. Exergy analysis

The rate of exergy balance is written as follows (Dincer and Rosen, 2013a, b, c, d, e):

$$\sum_{in}\left(1 - \frac{T_0}{T_i}\right)\dot{Q}_i + \dot{W}_{in} + \sum_{in}\dot{m}_i ex = \sum_{out}\left(1 - \frac{T_0}{T_i}\right)\dot{Q}_i + \dot{W}_{out} + \sum_{out}\dot{m}_i ex + \dot{E}x_D \tag{33}$$

In the above equation, $\dot{E}x_D$ (W) is the exergy destruction,

$\sum_{in} \dot{m}_i \dot{ex}_i$ (W) is the sum of the input exergy rates, $\sum_{out} \dot{m}_i \dot{ex}_i$ (W) is the sum of the output exergy rates and $\frac{T_0}{T_i}$ is the ratio of the ambient temperature to the flow temperature.

The exergy rate balance and exergy efficiency for the various components of the system are shown in Table 1 (Ghorbani et al., 2018; Shirmohammadi et al., 2018).

In the above table, subscripts 1 to 9 show the location considering Fig. 1. D means destruction. PV, FC, and C mean photovoltaic, fuel cell and compressor, respectively, and subscript ex means exergy.

$\dot{E}x_{10,solar}$(W) is the input exergy rate of solar beams to photovoltaic cells and it can be calculated by Kelly et al. 2009:

$$\dot{E}x_{10,solar} = A_{PV} I \left[1 - 1.33 \left(\frac{T_0}{T_s} \right) + 0.33 \left(\frac{T_0}{T_s} \right)^4 \right] \tag{34}$$

where A_{PV} (m^2) is the area of the photovoltaic cell, I (W/m^2) is the amount of received radiation by photovoltaic cell, T_0 (K) is the ambient temperature,T_s (K) is the sun temperature and it is assumed to 5780 K.

The system energy and exergy efficiencies are calculated by:

$$\eta_{en,sys} = \frac{\dot{W}_{FC} - \dot{W}_c}{IbA_{pv} + \dot{m}_2 h_2} \tag{35}$$

$$\eta_{ex,sys} = \frac{\dot{W}_{FC} - \dot{W}_c}{\dot{E}x_{10} + \dot{E}x_2} \tag{36}$$

$\eta_{en,sys}$ and $\eta_{ex,sys}$ are system energy and exergy efficiencies.

2.3. Economic analysis

The electricity cost is calculated by (Charles T. Horngren, 2016; Frangopoulos, 1987):

$$CE = \frac{C_I * \frac{(1+i)^n}{(1+i)^n - 1} + C_{O\&M}}{\text{Yearly Generated Energy} * c_f} \tag{37}$$

where n presents the project's lifetime (25 years), C_I ($) is the initial investment cost,$C_{O\&M}$ ($) is the maintenance cost, c_f is the system capacity factor and i is the bank interest rate (3%).

2.4. Advanced exergy analysis

In advanced exergy analysis, we have two parts of exergy destruction. One part is due to its irreversibility, which is known as the endogenous exergy destruction. The second part is due to the ineffectiveness of other components of the system that applies to this component; which is known as the exogenous exergy destruction. With the separation of the exergy destruction, our understanding of the effect of each component function is higher and the interaction between the components is clarified. With this method, it can be determined that the amount of exergy destruction is related to the equipping itself and how much does it relate to other equipment's in the cycle. (Bagheri et al., 2019; Kelly et al., 2009):

$$CE = \frac{C_I * \frac{(1+i)^n}{(1+i)^n - 1} + c_{O\&M}}{Yearly\ Generated\ Energy * c_f} \tag{38}$$

where superscripts EN and EX are presented as endogenous and exogenous respectively.

Part of the destruction of exergy in a component due to production methods and industrial constraints is inevitable. The remaining part is avoidable and it can be eliminated or at least minimized. So the exergy destruction of each component is divided into avoidable and unavoidable parts. In fact, the avoidable exergy destruction can be improved. For example, for photovoltaic system, the amount of exergy destruction that is related to solar radiation beam is evitable. But the exergy destruction that is related to material used in photovoltaic cells (for example reduction efficiency of photovoltaic cells with increasing temperature) can be improved (Bagheri et al., 2019; Kelly et al., 2009):

$$\dot{E}_{D,K} = \dot{E}_{D,K}^{UV} + \dot{E}_{D,K}^{AV} \tag{39}$$

In the above equation AV and UV subscript represent avoidable and unavoidable terms, respectively.

Advanced exergy analysis, in addition to dividing the exergy destruction into two parts, endogenous and exogenous, classifies each of these divisions into two avoidable and unavoidable terms. Thus, the exergy destruction of each component is divided into four parts; unavoidable endogenous, avoidable endogenous, unavoidable exogenous and avoidable exogenous terms, and it can be calculated by (Bagheri et al., 2019; Kelly et al., 2009):

$$\dot{E}_{D,K} = \dot{E}_{D,K}^{EN,UN} + \dot{E}_{D,K}^{EN,AV} + \dot{E}_{D,K}^{EX,UN} + \dot{E}_{D,K}^{EX,AN} \tag{40}$$

So in advanced exergy analysis, the exergy destruction of each component is divided to four parts. Two of these parts are evitable that they can be improved by optimization of cycle, promotion of material used, etc. Two of them are inevitable due to physical restrictions. For example, the energy efficiency of internal combustion (IC) engines cannot increase Carnot efficiency.

3. Results and discussion

Tehran is the capital of Iran which is geographically located at 51° 17′ to 51° 33′ in the East, 35° 36′ to 35° 44′ in the North (en.wikipedia.org/wiki/Tehran) (Mohammadi and Mehrpooya, 2019) (Mohammadi and Mehrpooya, 2019).

Table 1
The balance of exergy rate and exergy efficiency for the system components.

Components	Exergy rate balance	Exergy efficiency
Electrolyzer	$\dot{E}x_1 + \dot{E}x_2 = \dot{E}x_4 + \dot{E}x_3 + \dot{E}x_{D\ electrolyzer}$	$\eta_{ex\ electrolyzer} = \frac{\dot{E}x_4}{\dot{E}x_1 + \dot{E}x_2}$
Compressor	$\dot{W}_c + \dot{E}x_4 = \dot{E}x_6 + \dot{E}x_{D\ c}$	$\eta_{ex,\ c} = \frac{\dot{E}x_6}{\dot{W}_c + \dot{E}x_4}$
Fuel cell	$\dot{E}x_7 = \dot{W}_{FC} + \dot{E}x_9 + \dot{E}x_{D,FC}$	$\eta_{ex,FC} = \frac{\dot{W}_{FC}}{\dot{E}x_7}$
Photovoltaic cell	$\dot{E}x_{10,solar} = \dot{W}_{PV} + \dot{E}x_{D,PV}$	$\eta_{ex,\ PV} = \frac{\dot{W}_{PV}}{\dot{E}x_{10}}$

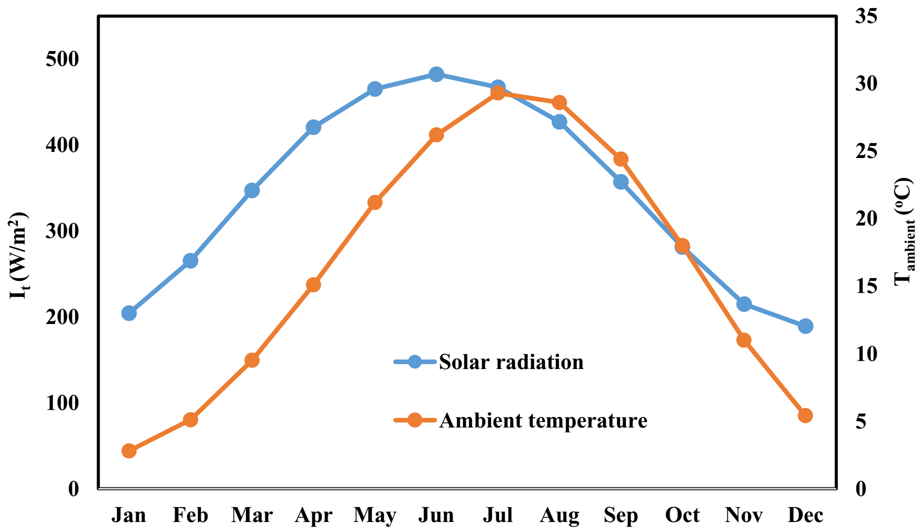

Fig. 2. Average monthly solar radiation and air temperature for the city of Tehran.

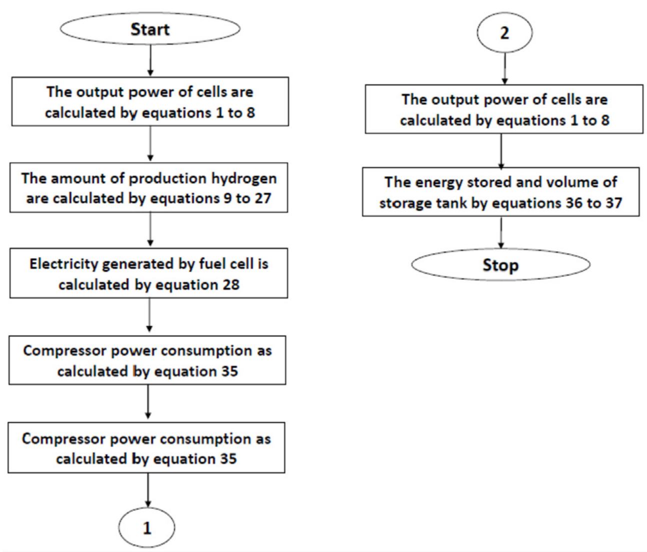

Fig. 3. Flow chart of solving the equations.

The average monthly radiation and average air temperature values for the city of Tehran are presented in Fig. 2 (www.weather.ir) (Patel et al., 2017) (Patel et al., 2017). In Fig. 3 the flowchart for solving the equations is presented. For mathematical modeling of this system, one program is written in MATLAB software. This program follows the flow chart that is shown in Fig. 3. For calculation the thermodynamic properties of water and hydrogen, the Refprop software is used.

In Fig. 4 the results of this study are compared with reference results (Molavi dariani et al., 2007). The reason for the small difference in the results is due to the application of different voltage drop equation.

For validation of the results, the data of reference (Ismail et al., 2019) is considered. In reference (Ismail et al., 2019), a photovoltaic system with PEM electrolyzer is installed in Suez city, Egypt.

Fig. 23 of this reference shows the hydrogen flow rate production during different hours of 21 th March 2016 in Suez city.

For comparison the results, the data of this reference is inserted to the code as inlet information. Fig. 5 shows the comparison between the data of reference (Ismail et al., 2019) with the results of the model developed for this paper.

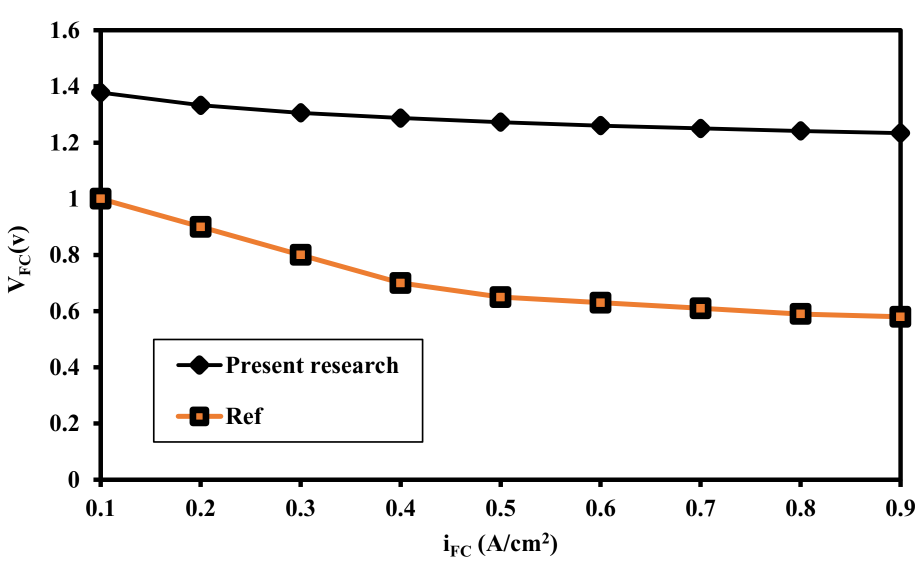

Fig. 4. Validation of the results with reference.

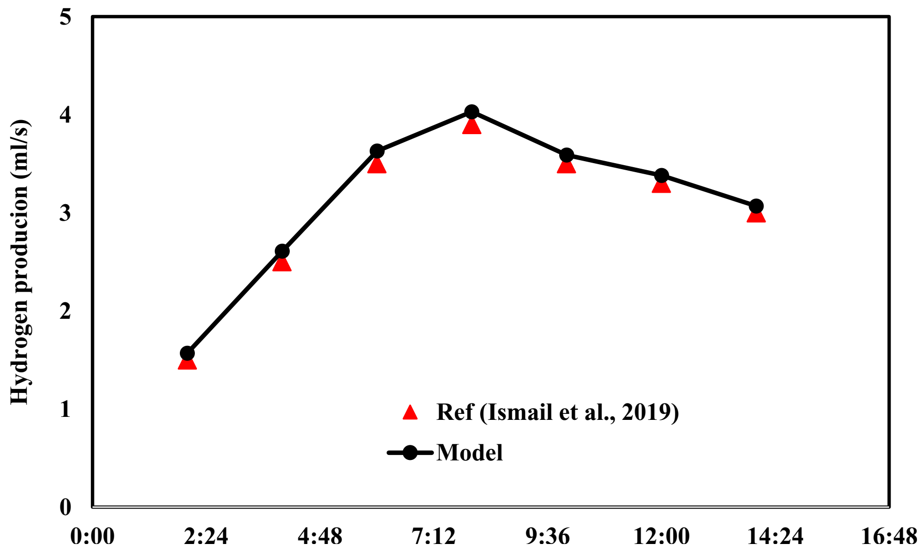

Fig. 5. Comparison between the data of reference (Ismail et al., 2019) with the results of the model.

In Table 2, system design specifications are presented. The price of the system components is presented in Table 3 (B. D. James, 2016; G. Parks, 2014; Schmidt et al., 2017).

The cost of operation and maintenance is assumed to be 3% of the initial installation cost. Characteristics of photovoltaic cells used in this study are shown in Table 4. Table 4 corresponds to the technical specifications of the poly group ND module of Sharp Company (Model: NU-A188EY). This type of module has the maximum power of 188 W and 48 cells, with a total area of 0.0245 m^2 per cell in this simulation (Origin Energy) (Shirmohammadi et al., 2015).

Average monthly electrical power production by the photovoltaic cell is shown in Fig. 6. Electrical power production by the photovoltaic cell is consistent with solar radiation (Fig. 2).

The maximum monthly average electrical power production by photovoltaic cell is 6810 W in June. The minimum value of electrical power production is 2670 W in December. The standard deviation of electrical power production is equal to 4140W, which is a considerable amount. In three months of May, June and July, the maximum electrical power production is produced.

Fig. 7 shows the hydrogen production and water consumption of the system for different months of a year. Maximum value of hydrogen production is 158 kg/month in June and the minimum value is equal to 62.1 kg/month in December. Similar to Fig. 5, the

Table 2
System design specification.

System specification	Values
Area of photovoltaic module (m^2)	2.16
Number of photovoltaic cell modules	64
Cell angle ratio (Degree)	30
Tank volume (m^3)	0.8
compressor pressure ratio	10
Fuel cell temperature (K)	338
Fuel cell pressure (kPa)	200
The area of each sheet of fuel cell (cm^2)	100
Number of fuel cell sheets	70
Fuel cell current density (A/cm^2)	1.8
Fuel cell voltage (V)	0.8

Table 3
Cost of system components.

Components	Investment cost ($)
Photovoltaic cells	212 per module
Electrolyzer	1.86 per W
Compressor	1.7 per W
Hydrogen tank	1.9 per m^3

Table 4
The characteristic of photovoltaic cells.

Model	ND195R1s
Max power at standard condition	188 W
Rectified voltage at standard condition	1000 V_{DC}
Voltage at max power and standard condition	23.66 V
Current at max power and standard condition	8.27 A
Open circuit voltage at standard condition	29.6 V
Short circuit current at standard condition	8.6 A
Max allowable current at standard condition	15 A
Allowable temperature range	−40–90 °C
Nominal temperature	47.5 °C
Efficiency	14.24%
Output power fault	5%
Cell number per module	48
Cell size	156.5*156.5 mm^2
Diameter of front glass	3 mm
Weight	16.5 kg

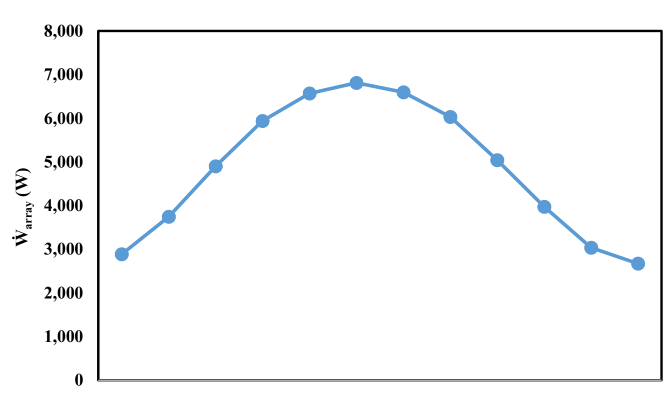

Fig. 6. The average monthly electrical power production by the photovoltaic cells.

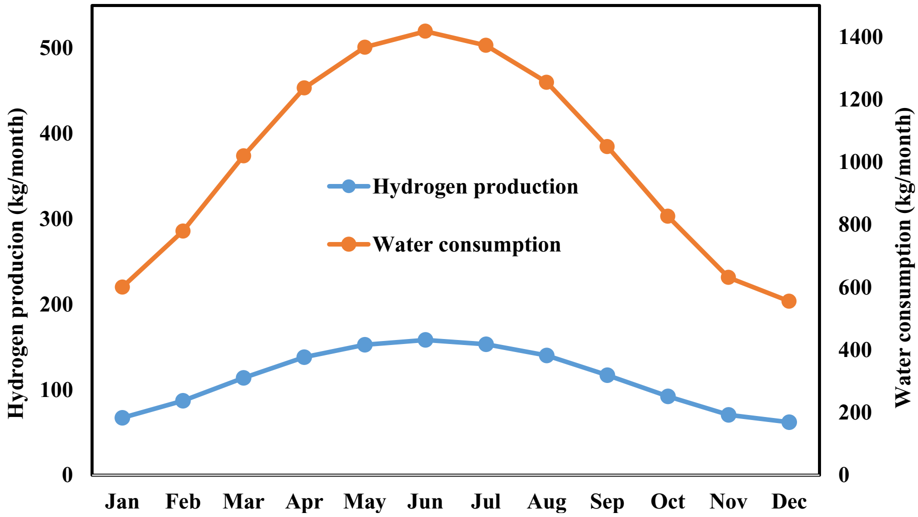

Fig. 7. The monthly average hydrogen production and water consumption by the studied system.

maximum and minimum values are in June and December, respectively.

Fig. 8 shows the monthly average of system energy efficiency where the highest energy efficiency is in January and December months.

Perhaps at first glance, the highest energy efficiency should be in the months that have the highest solar radiation, while the opposite is observed. In the cold seasons of the year, although the solar radiation is low, the efficiency of the fuel cell and the photovoltaic cell is increased due to the decrease in temperature. On the other hand, the denominator energy efficiency (equation (35)) is reduced in cold seasons. So, the sum of these effects results in higher energy efficiency in cold months than hot months. In general, we can also conclude that for the proposed system efficiency, the temperature is a more important factor than solar radiation.

Fig. 9 is the monthly average of the overall exergy efficiency of the system. The trend of change is similar to energy efficiency. Fig. 10 shows the annual exergy destruction for different components of the system.

Maximum and minimum exergy destruction rates are related to photovoltaic cells and compressor. Since in photovoltaic cells, we have a large amount of inlet exergy (equation (36)) from the sun, a large amount of this exergy is wasted in the photovoltaic cells. In electrolyzer and fuel cell, also the considerable exergy destructions are seen due to the chemical reaction in these components.

The price of electricity produced by the system is estimated to be 0.127 $/kWh. Fig. 11 shows the comparison of this price with other electricity costs produced by other renewable energy resources (Bahiraei et al., 2019) (Bahiraei et al., 2019).

Electricity cost of this system is lower than the electricity cost produced by offshore wind turbine and solar thermal and it is higher than the other renewable resources shown in Fig. 11. Of course, this comparison is relative, because the exact calculation of electricity prices by renewable resources depends on several factors. These factors are the potential of the energy source in the area, the price of the desired power generation and the method of energy storage.

The cost of electricity of this system is higher than electrical cost

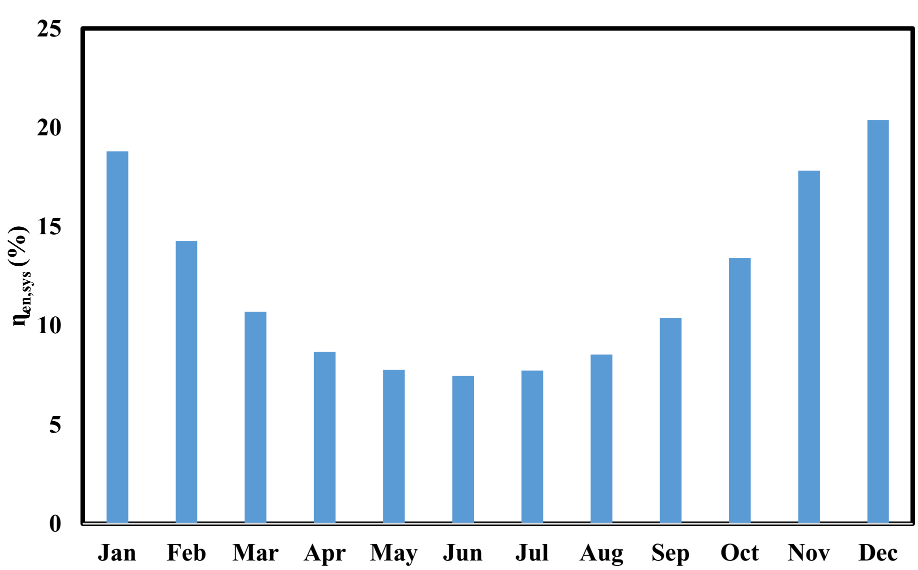

Fig. 8. The monthly average of the energy efficiency of the system.

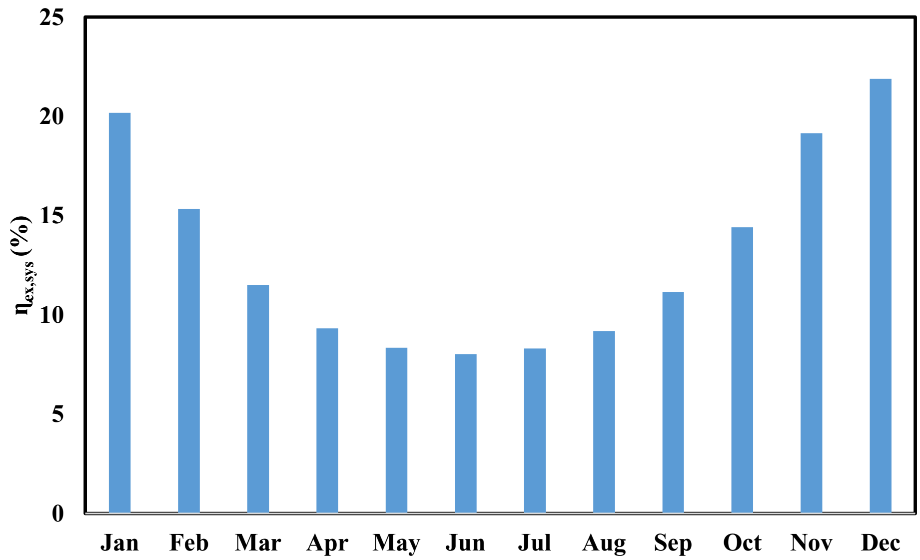

Fig. 9. The average monthly exergy efficiency of the system.

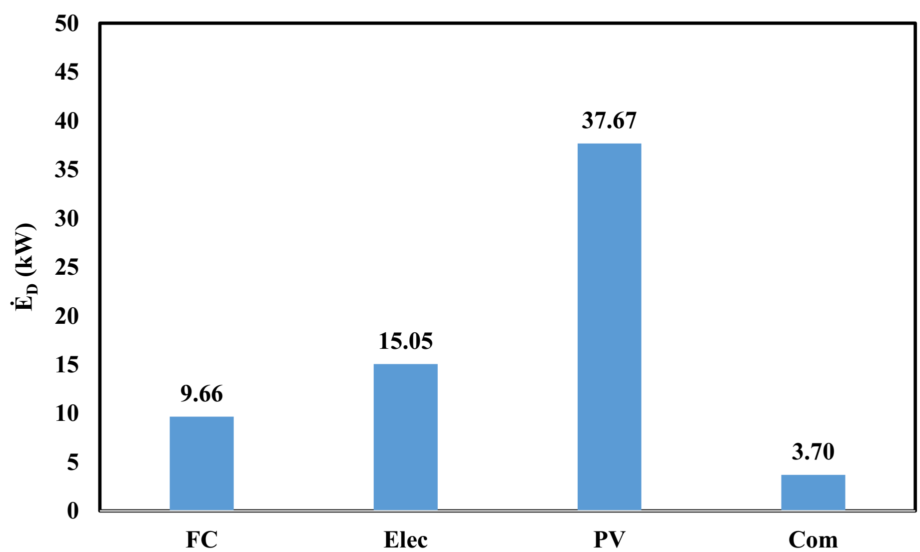

Fig. 10. The annual average value of exergy destruction for different system components.

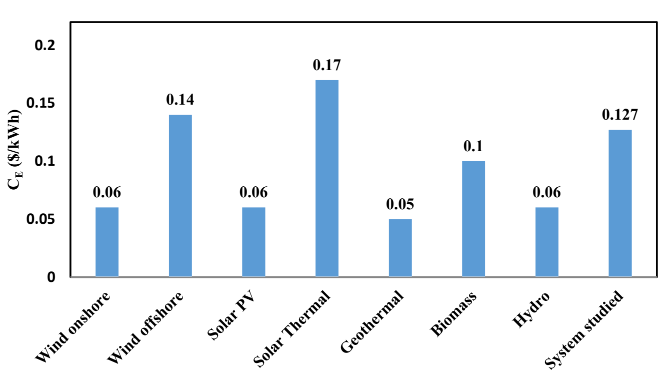

Fig. 11. Comparison of electricity cost for various renewable energy resource.

of centralized power plant, too. But for selection the best system, we should consider the following points:

1 The air pollution is a main problem of Tehran city. This system does not produce any air pollution in operation. So for selection this system or similar systems, we should also consider the social cost of air pollution.
2 Centralized power plant also has huge losses in electrical network (Both transfer and distribution). But this system can be used as a dispersed power generation system.
3 In remote area around Tehran, which the electrical power transmission is very hard or impossible. This system can be a choice. Since the potential of solar energy in Tehran is high.

Table 5 shows the values of endogenous unavoidable, endogenous avoidable, exogenous unavoidable and exogenous avoidable related to exergy destruction. Fig. 12 shows the percentage of avoidable and unavoidable endogenous and exogenous exergy destruction for total equipment's of a system.

In the photovoltaic cell, the major part of exergy destruction is related to unavoidable endogenous exergy destruction (%94.9). The reason is the dependence of inlet exergy of photovoltaic cell to

Table 5
Endogenous unavoidable, endogenous avoidable, exogenous unavoidable, and exogenous avoidable values for exergy destruction.

$\dot{E}_D$ (kW)	EN,UN	EN,AV	EX,UN	EX,AV	Total
PV	35.8	1.8	0	0	37.7
Elec	1.6	2.3	9.4	1.7	15.05
Com	0.56	0.26	2.28	0.6	3.7
FC	1.04	0.12	8.2	0.3	9.66

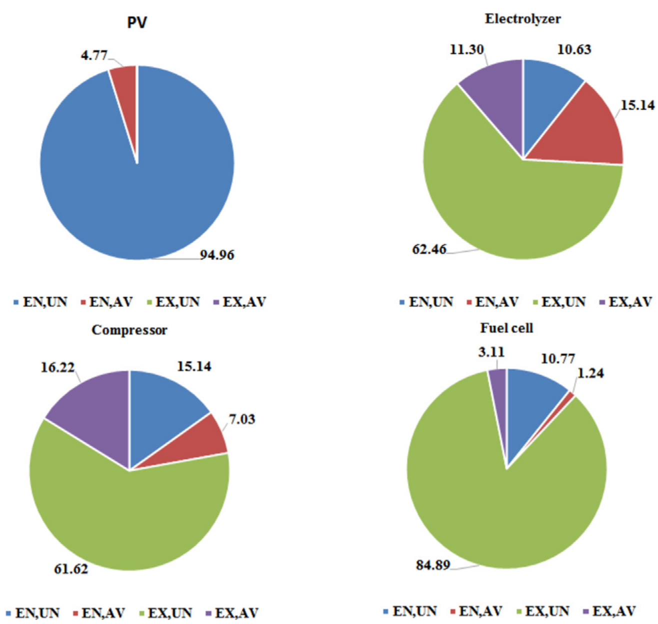

Fig. 12. Percent of avoidable and unavoidable endogenous and exogenous exergy destruction of total equipment of system.

ambient temperature sun temperatures and solar radiation (Equation (34)). These values cannot be optimized or changed by the manufacturers of photovoltaic cell. So it is unavoidable.

For calculation the exergy destruction avoidable and unavoidable exergy destruction rate, the following steps are considered:

1) Calculation the exergy destruction rate with $\dot{Ex}_{D,PV} = \dot{Ex}_{10,solar} - \dot{W}_{PV}$ in real condition
2) We assume the efficiency of photovoltaic cell is 100% and again the exergy destruction rate is calculated.
3) Difference between the values calculated in steps 1 and 2 is unavoidable exergy destruction rate. Because we cannot promote the efficiency of photovoltaic cells beyond 100%.
4) Difference between total exergy destruction and unavoidable exergy destruction is avoidable exergy destruction.
5) In photovoltaic cell, the exogenous exergy destruction is not existed. Since other components which is installed after photovoltaic do not have any effects on it.

In the electrolyzer, the major part of exergy destruction is related to exogenous unavoidable. Since the photovoltaic cells exergy destruction effects depend on the electrolyzer. Also by promoting the design and efficiency, 15% (2.3 kW) of electrolyzer exergy destruction can be reduced.

In the compressor, the major part of exergy destruction is related to exogenous unavoidable exergy destruction (61% or 2.28 kW). Also, the endogenous avoidable and unavoidable exergy destruction rates are 0. 26 kW (7.03%) and 0. 56 kW (15.14%), respectively. So for the compressor, we can reduce exergy destruction of about 7.0%.

In the PEM fuel cell, avoidable endogenous and exogenous exergy destructions are 10.8% and 3.1% of the total exergy destruction, respectively.

In general, in cycles whom their configurations are linear and they do not have a loop, previous equipment has considerable effects on exergy destruction of the next equipment.

4. Conclusion

This work presented the energy, exergy, advanced energy and economic analysis of hybrid system consisting of photovoltaic cells, electrolyzer and polymer electrolyte membrane fuel cell to provide a clean power to run an electrolyzer for hydrogen production. The produced hydrogen is compressed and then stored in a storage tank which is connected to the fuel cell for electricity production when needed. The proposed hybrid system is completely clean energy system with no greenhouse gas emissions. Using the thermodynamic and economic analyses, the main results f this work are summarized as:

- The highest average annual exergy destruction is in the photovoltaic cells as 37.67 kW and the lowest exergy destruction is in compressor as 3.7 kW, respectively.
- The minimum energy and exergy efficiencies are 7.5% and 8.2% in June, respectively.
- Electricity prices are competitive with the production of the offshore wind turbine and solar thermal cost of electricity.
- The maximum use of hydrogen and hydrogen production are 158 kg/month and 1420 kg/month in June, respectively.
- The highest value of unavoidable endogenous exergy destruction is in the photovoltaic cell as 94.9%.

According to the costs of components that are associated with the fuel cell and electrolyzer, the photovoltaic-hydrogen based system may become more attractive in future with the use of PEM based technology. Moreover, more recommended research based on this study should be investigated in the future, the parameters of such future research should include:

- PV material which results in better efficiency of the system for improved PV material
- Air pollution which results in a decreasing the system efficiency
- Types of hydrogen storage system which may include phase change material
- the system components can be optimized by using Particle Swarm Optimization to minimize the exergy destruction
- Life cycle analysis should be conducted

Nomenclature

A	Effective area cell (m^2)
C	Cost ($)

CE	Cost of electricity ($/kWh)
c_f	System capacity factor
C_p	Specific heat at constant pressure (kJ/kgK)
C_{O_2}	Oxygen concentration$(mol\ /cm^3\ )$
d	Distance between sun and earth (m)
e	Specific exergy (J/kg)
$\dot{E}$	Average output power (W)
$\dot{E}x$	Rate of exergy (W)
f	Reduction factor(96475 C)
F	Farady constant
$\overline{g}_f$	Specific Gibbs free energy
G	Gibbs free energy (kJ/kg)
G_{sc}	Solar constant equal to 1367 (W/m^2)
h	Specific enthalpy (kJ/kg)
H	Average solar radiation in equation (7)
H	Enthalpy (kJ/kmol)
i_{FC}	Electricity current density of the fuel cell (A/m^2)
I_b	Solar radiation (W/m^2)
J	Current density (mA/cm^2)
k	Ratio of specific heat $\left(k = \frac{C_P}{C_V}\right)$
L	Longitude (Degree)
L	Membrane thickness (cm) in equation (22
$\dot{m}$	Mass flow rate (kg/s)
M	Mole production (mole/h)
M	Mass (kg) in Equation (33)
N	Number of Plate
n	Number of cells or Equipment life (Year) in Equation (42)
n	Number of days in equation (1)
$\dot{Q}$	Heat transfer rate (W)
R	Universal gas constant: 8.314 (J/molK)
R_C	Resistance of the electrodes against passing of electrons (Ω/cm)
R_M	Resistance of the electrolyte against the transit of ions (Ω/cm)
S	Defined parameter in equation (4)
S	Entropy (J/molK)
T	Temperature (^{o}C)
V	Volume (Lit) in Equation (33)
V	Output Voltage (V)
$\dot{W}$	Power (W)

Greek Symbols

Δ	Difference
δ	Deflection angle (Degree)
θ_z	Zenith angle (Degree)
ω	Hour angle (Degree)
ϕ	Latitude (Degree)
η	Efficiency
θ	Attack angle (Degree)
γ	Temperature coefficient The absolute value of the energy temperature coefficient for each degree of increase of 25 °C
ρ_M	Specific resistance of the membrane (Ω.cm)
ζ	Model parameter in Equation (32)

Subscripts

AV	Avoidable
aday	Average temperature of day
array	photovoltaic array area
b	Beam
celleff	Average temperature of cell
c	Compressor
dirt	Pollution
D,K	Destruction for component K
elz	Electrolyze
ensys	Energy of the system
exsys	Exergy of the system
ex	Exergy
EN	Endogenous
EX	Exogenous
FC	Fuel cell
H_2O	Water
H_2	Hydrogen gas
I	Initial
in	Input
man	Manufacturer
max	Maximum
O&M	Operation and maintenance
out	Output
O_2	Oxygen gas
PV	Photovoltaic
product	Product
reactant	Reactant
rev	Reversible
sys	System
tank	Storage tank
temp	Temperature
theo	Theoretical
tilt	Tilt of panel
UV	Unavoidable
V	Voltage

References

Abadlia, I., Adjabi, M., Bouzeria, H., 2017. Sliding mode based power control of grid-connected photovoltaic-hydrogen hybrid system. Int. J. Hydrogen Energy 42 (47), 28171–28182.

Arsalis, A., Alexandrou, A.N., Georghiou, G.E., 2018. Thermoeconomic modeling of a completely autonomous, zero-emission photovoltaic system with hydrogen storage for residential applications. Renew. Energy 126, 354–369.

Ashari, G., Ehyaei, M., Mozafari, A., Atabi, F., Hajidavalloo, E., Shalbaf, S., 2012. Exergy, economic, and environmental analysis of a PEM fuel cell power system to meet electrical and thermal energy needs of residential buildings. J. Fuel Cell Sci. Technol. 9 (5), 051001.

Babayan, M., Mazraeh, A.E., Yari, M., Niazi, N.A., Saha, S.C., 2019. Hydrogen production with a photovoltaic thermal system enhanced by phase change materials, Shiraz, Iran case study. J. Clean. Prod. 215, 1262–1278.

Bagheri, B.S., Shirmohammadi, R., Mahmoudi, S.M.S., Rosen, M.A., 2019. Optimization and comprehensive exergy-based analyses of a parallel flow double-effect water-lithium bromide absorption refrigeration system. Appl. Therm. Eng. 152, 643–653.

Bahiraei, M., Salmi, H.K., Safaei, M.R., 2019. Effect of employing a new biological nanofluid containing functionalized graphene nanoplatelets on thermal and hydraulic characteristics of a spiral heat exchanger. Energy Convers. Manag. 180, 72–82.

Baik, M., Hammoudi, M., Salhi, Y., Kirati, S.K., 2018. Hydrogen production by hybrid system and its conversion by fuel cell in Algeria; Djanet. Int. J. Hydrogen Energy 43 (6), 3466–3474.

Bakelli, Y., Hadj Arab, A., Azoui, B., 2011. Optimal sizing of photovoltaic pumping system with water tank storage using LPSP concept. Sol. Energy 85 (2), 288–294.

Barbir, F., Gómez, T., 1997. Efficiency and economics of proton exchange membrane (PEM) fuel cells. Int. J. Hydrogen Energy 22 (10), 1027–1037.

Bilgen, E., 2004. Domestic hydrogen production using renewable energy. Sol. Energy 77 (1), 47–55.

Bizon, N., Thounthong, P., 2018. Fuel economy using the global optimization of the fuel cell hybrid power systems. Energy Convers. Manag. 173, 665–678.

Bukar, A.L., Tan, C.W., 2019. A review on stand-alone photovoltaic-wind energy system with fuel cell: system optimization and energy management strategy. J. Clean. Prod. 221, 73–88.

Charles, T., Horngren, S.M.D., Rajan, Madhav V., 2016. Cost Accounting: A Managerial Emphasis. Prentice Hal.

Da Silva, E.P., Marin Neto, A.J., Ferreira, P.F.P., Camargo, J.C., Apolinário, F.R., Pinto, C.S., 2005. Analysis of hydrogen production from combined photovoltaics, wind energy and secondary hydroelectricity supply in Brazil. Sol. Energy 78 (5), 670–677.

Dahbi, S., Aziz, A., Messaoudi, A., Mazozi, I., Kassmi, K., Benazzi, N., 2018. Management of excess energy in a photovoltaic/grid system by production of clean

hydrogen. Int. J. Hydrogen Energy 43 (10), 5283–5299.
Dincer, I., Rosen, M.A., 2013a. Chapter 1 - thermodynamic fundamentals. In: Dincer, I., Rosen, M.A. (Eds.), Exergy, second ed. Elsevier, pp. 1–20.
Dincer, I., Rosen, M.A., 2013b. Chapter 2 - exergy and energy analyses. In: Dincer, I., Rosen, M.A. (Eds.), Exergy, second ed. Elsevier, pp. 21–30.
Dincer, I., Rosen, M.A., 2013c. Chapter 11 - exergy analysis of renewable energy systems. In: Dincer, I., Rosen, M.A. (Eds.), Exergy, second ed. Elsevier, pp. 193–259.
Dincer, I., Rosen, M.A., 2013d. Chapter 17 - exergy analysis of hydrogen production systems. In: Dincer, I., Rosen, M.A. (Eds.), Exergy, second ed. Elsevier, pp. 347–362.
Dincer, I., Rosen, M.A., 2013e. Chapter 18 - exergy analysis of fuel cell systems. In: Dincer, I., Rosen, M.A. (Eds.), Exergy, second ed. Elsevier, pp. 363–382.
Ezzat, M.F., Dincer, I., 2016. Development, analysis and assessment of a fuel cell and solar photovoltaic system powered vehicle. Energy Convers. Manag. 129, 284–292.
Frangopoulos, C.A., 1987. Thermo-economic functional analysis and optimization. Energy 12 (7), 563–571.
Ghorbani, B., Mehrpooya, M., Shirmohammadi, R., Hamedi, M.-H., 2018. A comprehensive approach toward utilizing mixed refrigerant and absorption refrigeration systems in an integrated cryogenic refrigeration process. J. Clean. Prod. 179, 495–514.
Hwang, J.J., Lai, L.K., Wu, W., Chang, W.R., 2009. Dynamic modeling of a photovoltaic hydrogen fuel cell hybrid system. Int. J. Hydrogen Energy 34 (23), 9531–9542.
Ismail, T.M., Ramzy, K., Elnaghi, B.E., Abelwhab, M.N., El-Salam, M.A., 2019. Using MATLAB to model and simulate a photovoltaic system to produce hydrogen. Energy Convers. Manag. 185, 101–129.
James, B.D., H, C., Huya-Kouadio, J.M., DeSantis, D.A., 2016. Final Report: Hydrogen Storage System Cost Analysis.
John, A., Duffie, W.A.B., 2013. Solar Engineering of Thermal Processes, 4 ed. John wiley and sons.
Kelly, S., Tsatsaronis, G., Morosuk, T., 2009. Advanced exergetic analysis: approaches for splitting the exergy destruction into endogenous and exogenous parts. Energy 34 (3), 384–391.
Khemariya, M., Mittal, A., Baredar, P., Singh, A., 2017. Cost and size optimization of solar photovoltaic and fuel cell based integrated energy system for un-electrified village. J. Energy Storage 14, 62–70.
Levene, J.I., Mann, M.K., Margolis, R.M., Milbrandt, A., 2007. An analysis of hydrogen production from renewable electricity sources. Sol. Energy 81 (6), 773–780.
Maleki, A., Pourfayaz, F., Ahmadi, M.H., 2016. Design of a cost-effective wind/photovoltaic/hydrogen energy system for supplying a desalination unit by a heuristic approach. Sol. Energy 139, 666–675.
Mitlitsky, F., Myers, B., Weisberg, A.H., 1998. Regenerative fuel cell systems. Energy Fuels 12 (1), 56–71.
Mohammadi, A., Mehrpooya, M., 2019. Thermodynamic and economic analyses of hydrogen production system using high temperature solid oxide electrolyzer integrated with parabolic trough collector. J. Clean. Prod. 212, 713–726.
Molavi dariani, A., Rastegar, H., Ghadimi, A.A., 2007. Providing a Precise Model for a Polymer Electrolyte Fuel Cell Considering the Effect of Temperature, 22nd International Power System Conference. Tavanir, Power Research Institute, Tehran, Iran, pp. 3–12.
Origin Energy, Link: www.originenergy.com.au, Last Accessed Date: 23.06.2019.
Parks, G., R.B., Cornish, J., Remick, R., 2014. Hydrogen Station Compression, Storage, and Dispensing Technical Status and Costs (Technical report).
Patel, B., Desai, N.B., Kachhwaha, S.S., Jain, V., Hadia, N., 2017. Thermo-economic analysis of a novel organic Rankine cycle integrated cascaded vapor compression–absorption system. J. Clean. Prod. 154, 26–40.
Petrakopoulou, F., Robinson, A., Loizidou, M., 2016. Exergetic analysis and dynamic simulation of a solar-wind power plant with electricity storage and hydrogen generation. J. Clean. Prod. 113, 450–458.
Rekioua, D., Bensmail, S., Bettar, N., 2014. Development of hybrid photovoltaic-fuel cell system for stand-alone application. Int. J. Hydrogen Energy 39 (3), 1604–1611.
Saidi, M., Abbassi, A., Ehyaei, M., 2005a. Exergetic optimization of a PEM fuel cell for domestic hot water heater. J. Fuel Cell Sci. Technol. 2 (4), 284–289.
Saidi, M.H., Ehyaei, M.A., Abbasi, A., 2005b. Optimization of a combined heat and power PEFC by exergy analysis. J. Power Sources 143 (1), 179–184.
Schmidt, O., Gambhir, A., Staffell, I., Hawkes, A., Nelson, J., Few, S., 2017. Future cost and performance of water electrolysis: an expert elicitation study. Int. J. Hydrogen Energy 42 (52), 30470–30492.
Shirmohammadi, R., Ghorbani, B., Hamedi, M., Hamedi, M.-H., Romeo, L.M., 2015. Optimization of mixed refrigerant systems in low temperature applications by means of group method of data handling (GMDH). J. Nat. Gas Sci. Eng. 26, 303–312.
Shirmohammadi, R., Soltanieh, M., Romeo, L.M., 2018. Thermoeconomic analysis and optimization of post-combustion CO2 recovery unit utilizing absorption refrigeration system for a natural-gas-fired power plant. Environ. Prog. Sustain. Energy 37 (3), 1075–1084.
Smaoui, M., Abdelkafi, A., Krichen, L., 2015. Optimal sizing of stand-alone photovoltaic/wind/hydrogen hybrid system supplying a desalination unit. Sol. Energy 120, 263–276.
Yadav, D., Banerjee, R., 2018. Economic assessment of hydrogen production from solar driven high-temperature steam electrolysis process. J. Clean. Prod. 183, 1131–1155.